◆ Human Brain Mapping 21:34–43(2004) ◆

TECHNICAL REPORT

Evaluating Requirements for Spatial Resolution of fMRI for Neurosurgical Planning

Seung-Schik Yoo,[1] Ion-Florin Talos,[2] Alexandra J. Golby,[2] Peter McL. Black,[2] and Lawrence P. Panych[1]*

[1]*Department of Radiology, Brigham and Women's Hospital, Harvard Medical School, Boston, Massachusetts*
[2]*Department of Neurosurgery, Brigham and Women's Hospital, Harvard Medical School, Boston, Massachusetts*

Abstract: The unambiguous localization of eloquent functional areas is necessary to decrease the neurological morbidity of neurosurgical procedures. We explored the minimum spatial resolution requirements for functional magnetic resonance imaging (fMRI) data acquisition when brain mapping is used in neurosurgical planning and navigation. Using a 1.5 Tesla clinical MRI scanner, eight patients with brain tumors underwent fMRI scans using spatial resolution of approximately $4 \times 4 \times 4$ mm^3 to map the eloquent motor and language areas during the performance of cognitive/sensorimotor tasks. The fMRI results were then used intra-operatively in an open MRI system to delineate eloquent areas. Retrospectively, activation patterns were visually inspected by a neurosurgeon to determine qualitatively whether ambiguity with respect to the activation boundaries, due to low spatial resolution, could be of potential significance for surgical guidance. A significant degree of ambiguity in both the extent and shape of activation was judged to be present in data from six of the eight patients. Analysis of fMRI data at multiple resolutions from a normal volunteer showed that at 3 mm isotropic resolution, eloquent areas were better localized within the gray matter although there was still some potential for ambiguity caused by activations appearing to cross a sulcus. The data acquired with 2-mm isotropic voxels significantly enhanced the spatial localization of activation to within the gray matter. Thus, isotropic spatial resolution on the order of $2 \times 2 \times 2$ mm^3, which is much higher than the resolutions used in typical fMRI examinations, may be needed for the unambiguous identification of cortical activation with respect to tumors and important anatomical landmarks. *Hum. Brain Mapp. 21:34–43, 2004.*

Key words: fMRI; brain mapping; neurosurgery; surgical planning; spatial resolution

INTRODUCTION

Due to its noninvasiveness and ability to provide relatively high spatial and temporal definition of cortical activation, functional MRI (fMRI) has been used in a wide variety of basic neuro-scientific investigations over the last decade. More recently, quantitative fMRI has emerged for such applications as studying the effect of pharmacological intervention and following the progression of neurological disorders [Cifelli and Matthews, 2002; Lowe et al., 2002]. Functional MRI has also been applied for pre-surgical func-

Contract grant sponsor: National Institutes of Health; Contract grant numbers: RO1 NS37992, P01 CA67165.

*Correspondence to: Dr. Lawrence P. Panych, Department of Radiology, Brigham and Women's Hospital, Harvard Medical School, 75 Francis St., Boston, MA 02115. E-mail: panych@bwh.harvard.edu

Received for publication 26 February 2003; Accepted 1 October 2003
DOI 10.1002/hbm.10148

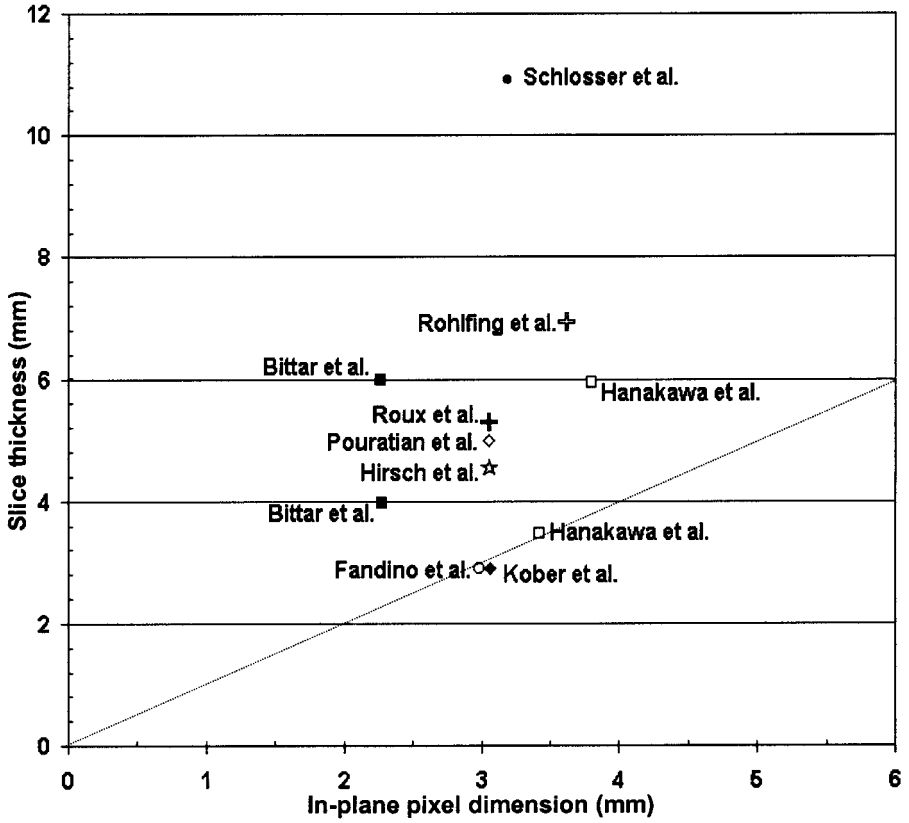

Figure 1.
Spatial resolutions used in recent fMRI investigations for neurosurgical planning. All studies used square pixel elements in the in-plane direction. Data plotted reflect effective spatial resolutions, including the effect of spatial smoothing and slice gap. The dotted line indicates isotropic voxels.

tional mapping of the brain and for intra-operative guidance [Bittar et al., 1999; Hirsch et al., 2000; Nimsky et al., 2001; Roux et al., 2001] and a number of studies validating fMRI results via direct cortical stimulation or optical recording have been performed [Fandino et al., 1999; Kober et al., 2001; Krings et al., 2001; Pouratian et al., 2002a,b].

In developing fMRI for neurosurgical planning, one confronts many challenges. First, the task paradigms should elicit robust activation in eloquent areas close to target lesions; however, they should also be able to be performed by patients who may have functional deficits due to those lesions. To safely maximize tumor resection, intraoperative electrophysiological mapping of the cerebral cortex, combined with preoperative functional imaging is desirable [Schiffbauer et al., 2001]. In order to do so, the fMRI data must be transformed and registered for presentation in the intra-operative environment. The paradigm itself should also be readily adapted to the intra-operative environment for potential cross validation of the functional areas under awake-surgery.

A further important challenge in fMRI is insuring the spatial accuracy of the activation patterns. Precise definition of the activation boundaries in neurosurgical planning is necessary because of the possibility that eloquent cortical areas are invaded during surgical procedures and neurological deficits result. In fact, studies have shown that histologically abnormal tissues may even show function within the tumor itself [Ojemann et al. 1996; Skirboll et al. 1996]. The spatial resolution used when acquiring fMRI data limits the inherent precision of fMRI for delimiting eloquent areas, thus high special resolution would seem to be favorable for such studies. However, the sensitivity of fMRI for detecting activation may actually decrease significantly if spatial resolution is set too high [Yoo et al., 2001]. It is, therefore, important to determine the exact requirements for spatial resolution, taking into account the intended application.

The limit of spatial resolution for fMRI is determined by a complicated interplay of many study parameters such as temporal resolution, the duration of the overall scan session, volume to be covered, magnetic field strength, and type of MRI sequence. A review of recent fMRI studies for neurosurgical planning (Fig. 1), shows that several fMRI studies have been conducted (within a limited field-of-view [FOV]) at a spatial resolution that would be considered relatively high for fMRI studies, i.e., with voxel sizes as small as $3 \times 3 \times 3$ mm^3 [Fandino et al., 1999; Kober et al., 2001]. However, there are no reports of systematic studies that have demonstrated the need or advisability of using high spatial resolution for pre-surgical functional mapping. In general, it seems that the spatial resolution parameters used for most fMRI studies have been derived from protocols used for normal subject studies, i.e., 5- to 6-mm slice thickness, often covering the whole brain with an in-plane resolution of 3 to 4 mm [Hanakawa et al., 2001; Rohlfing et al., 2000; Schlosser et al., 1999].

TABLE I. Brain tumor patient information, history, and neurological findings

Age (yr)/ gender	Tumor location	Diagnosis	fMRI task	History and neurological findings
33/F	Left SFG & PrCG	Suspicous low-grade glioma	Motor tasks	Focal seizures with slight weakness/ lack of coordination of the right hand
34/F	Right temporal lobe	Oligodendroglioma WHO II/IV	Language task	History of brain tumor biopsy and radiation therapy with presence of generalized seizures
58/F	Left mSFG & SFG	Oligodendroglioma WHO II/IV	Motor tasks	No neurological deficits
64/M	Medial aspect of left PrCG	Anaplastic glioma	Motor tasks	Recurrent tumor with history of radiation therapy and moderate left leg monoparesis
39/M	Left PrCG	Oligodendroglioma WHO II/IV	Motor and Language tasks	Recurrent generalized seizures
59/M	Right parieto-occipital lobe	Metastastic melanoma	Motor and Language tasks	No neurological deficits
44/F	Right fronto-parietal lobe	Recurrent anaplastic astrocytoma	Motor tasks	Recurrent tumor with history of radiation therapy and moderate left hemiparesis
60/F	Right SFG & PrCG	Meningioma	Motor tasks	Recurrent generalized seizure with slight left hemiparesis

SFG, superior frontal gyrus; PrCG, precentral gyrus; mSFG, medial superior frontal gyrus.

Here we report results from eight brain tumor patients who underwent fMRI exams and subsequently had surgery in an open MRI system. The fMRI data in these studies were acquired at an intermediate, approximately isotropic spatial resolution of 4 mm. Activation patterns from the studies were examined following surgery by a neurosurgeon to determine qualitatively (regardless of whether ambiguity with respect to activation boundaries could be attributed to low spatial resolution) might have important ramifications for surgical guidance. In addition to the patient study, we also conducted a study examining data obtained from a normal subject performing several tasks, using different sets of spatial acquisition resolution parameters up to $2 \times 2 \times 2$ mm^3. In this study, we were motivated to investigate the utility of increasing the spatial resolution much higher than the resolution commonly used for typical applications for studying normal cognitive functions. This is the first report, to our knowledge, of an attempt to specifically address spatial resolution with respect to the precision of functional localization for surgical planning.

PATIENTS AND METHODS

fMRI of Surgical Patients

Patients

Pre-operative functional mapping studies were performed on eight patients (5 women, 3 men, mean age 48.9 ±12.7 years). Information about tumor location, primary diagnosis, and brief medical history is given in Table I. All patients who participated in the study gave written consent according to guidelines set forth by our local Institutional Review Board. Two separate imaging examinations were conducted for each patient: an anatomical imaging session and a functional imaging session. All exams were performed on a 1.5T clinical MR scanner (GE Medical Systems, Milwaukee, WI) with enhanced gradient hardware.

Anatomical MRI

In the anatomical imaging session, the following whole-brain image sets were acquired: (1) a 3D-Spoiled Gradient Recalled (SPGR) sequence with 1.5-mm sagittal slices, TE/TR = 6/35 msec, FA = 75 degrees, FOV = 24 cm, matrix = 256 × 256; (2) a T2-weighted fast-spin-echo series with 5-mm axial slices, TE/TR = 100/3,000 msec, FOV = 22 cm, matrix = 256 × 192; and (3) a phase-contrast MR angiographic sequence with 1.5-mm sagittal slices, TR = 32 msec, FA = 20 degrees, FOV = 24 cm, matrix = 256 × 128, V_{enc} = 60. From these sets, gray matter, white matter, and CSF were segmented along with tumor and venous structures using software developed at our institution. Pre- and post-contrast T1-weighted images were also acquired to detect enhancing tumor tissue. In some cases, localized diffusion-tensor and proton spectroscopic data were acquired in the vicinity of the tumor.

Functional MRI

Each fMRI session began with the acquisition of a T1-weighted 3-plane localizer series. Following the acquisition of localizers, reference anatomical images were then acquired covering the same slice locations as the echo-planar imaging (EPI). These reference images were used to determine parameters for co-registering fMRI results with the

high-resolution T1-weighted anatomical images acquired in the anatomical imaging session. For each fMRI run, EPI data were acquired from 22 axial slices (thickness 4 mm) covering the surgical field. Parameters of the EPI sequence were TR/TE = 2,000/50 msec, FA = 90 degrees, FOV = 24 cm, matrix = 64 × 64. The voxel size was 3.75 × 3.75 × 4 mm^3, slightly less than the maximum spatial resolution (3.12 × 3.12 × 3 mm^3) reported at 1.5T for presurgical functional imaging [Fandino et al., 1999]. The reference anatomical sequences were (1) a dual gradient-echo sequence with TE1/TE2/TR = MIN/50/2500 msec, 128 × 64 in-plane matrix and (2) a T1-weighted SPGR series with TE/TR = MIN/30 msec, FA = 30 degrees, 256 × 128.

Task Paradigms

Depending on the tumor location in the individual patients, primarily two different types of tasks were selected to map eloquent motor and language areas for the patient group (See Table I). For patients for whom the tumor was in an area where eloquent motor areas could be affected by surgery, hand-clenching tasks were performed. These tasks involved clenching the right and left hand separately and together. The clenching was paced at 1-Hz frequency using computer-generated auditory cues delivered via a MR-compatible headset (Avotec, Jesen Beach, FL). For mapping the language areas, a semantic language task (semantic determination of concrete vs. abstract nouns [Howard and Kahana, 2001]) was performed. The auditory cues/stimuli were delivered using the MR-compatible headset. In all fMRI runs, five task periods of 30-sec duration were interleaved with six 30-sec rest periods. The timing of auditory cues was controlled by Presentation software (Neurobehavioral Systems, CA).

Data processing

EPI data sets were reconstructed and then motion-corrected with respect to the first set of images using SPM99 (online at http://www.fil.ion.ucl.ac.uk/spm). Pixel-by-pixel paired *t*-test scores were calculated across the time course of the MR signal and converted to corresponding *P* values using in-house software. The functional data were then spatially registered to the high-resolution anatomical images using an approach based on maximization of mutual information [Wells et al., 1996]. The mis-registration between EPI and anatomical reference images was measured by matching the EP images to the second-echo image set acquired using the dual gradient-echo sequence. Images from the dual-echo sequence are T2*-weighted and have similar contrast to the EPI images. However, because the dual-echo images are not spatially distorted, correction parameters can be determined by measuring the spatial mismatch between them and the EPI images. EPI data were not spatially smoothed to retain the original spatial resolution.

Intra-operative mapping

Patients were operated in an open-configuration MRI system (Signa SP; GE Medical Systems, Milwaukee, WI) and underwent functional mapping using electro-cortical stimulation (ECS) during the surgical procedure. Prior to surgery, the fMRI *P* value results from the pre-operative imaging session were thresholded ($P < 10^{-6}$) and overlaid on anatomical images along with segmented tumor and vascular structures using 3D-slicer software [Gering et al., 2001]. In the intra-operative MRI system, reference anatomical images were acquired and co-registered to the 3-D slicer data. Using these co-registration parameters and real-time optical tracking (Flashpoint, Boulder, CO) of an Ojemann-type electrocortical stimulator, the location of the stimulator tip could be visualized by the surgeon in MRI data sets [Nabavi et al., 2001]. Thus, an intra-operative comparison of eloquent areas detected by ECS and those detected by fMRI could be made by the surgical team.

Post-operative assessment

After surgery, the fMRI mapping result was re-evaluated. A surgeon (not the operating surgeon) was asked to determine qualitatively whether ambiguity with respect to the activation boundaries could be of potential significance during the surgical guidance in any of the cases. In light of the individual surgeries, spatial features of activation were examined with respect to tumor boundaries and to location of the surgical field.

Multiresolution fMRI With Normal Subject

In addition to the patient studies, a series of fMRI investigations using different spatial-resolutions were performed on a healthy, right-handed 50-year-old male volunteer. The subject was free of neurologic and psychiatric disorders. A motor task (sequential finger tapping of the right hand, paced at 1-Hz frequency using computer-generated auditory cues) and a cognitive task (auditory word-comparison test where the subject was required to tap upon hearing a repeated word) were performed. Four 30-sec task periods were interleaved with five 30-sec control periods. Subject performance was monitored by using a motion-sensitive optical device attached to the tip of the second finger of the right hand.

In the fMRI sessions, three separate acquisition protocols were used with different spatial resolution parameters. Data was acquired at low, intermediate, and high resolution as detailed in Table II. Volume coverage and number of image acquisitions varied for each of the three protocols, however, the scan time was set equally to 4 min 30 sec for all runs. The data processing methods were the same as those used for the surgical patients and were applied for each of the three protocols. A lower statistical threshold ($P < 10^{-3}$) was used for the two higher resolution protocols than that used for the low-resolution protocol ($P < 10^{-6}$) due to the lower contrast-to-noise ratio of the higher resolution data.

In a separate processing stage, the 2-mm isotropic data was smoothed with a 3-D Gaussian kernel to have approximately the same resolution as the lowest resolution protocols in Table II (i.e., 3.75 × 3.75 × 6 mm^3 voxel size). Smoothing was followed by a processing step using the

TABLE II. Acquisition parameters for scan protocols employing different spatial resolutions

Protocol	Matrix size	Voxel size (in-plane × thickness), mm^3	TR (msec)	Slices (n)	Acquisitions (n)	Scans/epoch
Low	64 × 64	3.75 × 3.75 × 6	2500	24	108	12
Intermediate	80 × 80	3 × 3 × 3	3750	38	76	8
High	128 × 128	2 × 2 × 2	2500	19	108	12

same methods for detecting activation as were used for all other datasets. Functional activation patterns in the acquired low-resolution data and the smoothed data were qualitatively compared to see how closely activation patterns obtained using smoothed datasets matched the activation patterns obtained with data that were acquired directly.

The quality of the co-registration between the fMRI images and the high-resolution anatomical images was evaluated by examining the spatial overlap between the original EPI images and the anatomical images as demonstrated in Figure 2. Figure 2A shows a coronal section of the first set of EPI images acquired in the fMRI experiment. T2-weighting in the EPI sequence causes cerebrospinal fluid (CSF) to be bright in such an image. The EPI image was then thresholded to delineate the CSF space and overlaid on the anatomical reference image as shown in Figure 2B. To evaluate the co-registration, we now compare this overlay with Figure 2C, which shows the result of a segmentation of the T1-weighted reference image that locates CSF pixels. Comparing Figure 2B and 2C, we see a very close correspondence between CSF in the EPI image and CSF in the T1-weighted reference.

RESULTS

fMRI of surgical patients

Upon examination of patient data by a neurosurgeon, it was judged that significant ambiguity was present in the functional activation maps in six of the eight patients. Table III summarizes the cases and locations of relevance where the ambiguity was judged to be present. For example, activation was observed adjacent to the tumor boundaries, obscuring the exact delineation of areas of activation with respect to tumor boundaries (33/F, 58/F, and 60/F). This was considered significant for surgical guidance because eloquent tissue could not be unambiguously differentiated from tumor tissue. The second type of noted ambiguity consisted of activation profiles that appeared to cross a sulcus. This was considered significant because cortical tissue on either side of the sulcus could be determined as the optimal surgical corridor to the lesion.

TABLE III. Cases with ambiguity in delineating eloquent area with respect to the surgical field

Age/Gender	Regions-of-interest with ambiguity
33/F	Tumor margin near the border of left PrCG
58/F	Tumor margin at the border left SFG and anterior PrCG
60/F	Tumor margin at the border of mSFG
34/F	Inferior aspect of right STG and the superior aspect of right MTG
59/M	Central sulcus near hand motor area in PrCG
44/F	Superior frontal sulcus anterior to the PrCG

SFG, superior frontal gyrus; mSFG, medial superior frontal gyrus; PrCG, precentral gyrus; STG, superior temporal gyrus; MTG, middle temporal gyrus.

Figure 3 shows examples of activation observed adjacent to the tumor boundary obtained from Subject 1 (Fig. 3A,B) and Subject 2 (Fig. 3C,D). Subject 1 was a 33-year-old, right-handed female patient with a suspicious low-grade glioma near the left sensorimotor area. The patient concurrently had slight weakness and lack of coordination of the right hand. The patient later underwent intra-operative validation of the eloquent areas using cortical stimulation. Spatial overlap between the superior/posterior tumor margin and the activation profile are evident (Fig. 3A). Intraoperative cortical stimulation near the anterior aspect of the precentral gyrus (Fig. 3B) resulted in temporary arrests of hand motor function. Surgical removal of the tumor was approached from the latero-anterior aspect of the motor areas due to the eloquent motor areas surrounding the medial and posterior part of the tumor. The patient recovered from the surgery with a temporary post-operative motor deficit, which was later resolved.

Subject 2, a 34-year-old, left-handed female patient with a 3-month history of right temporal intra-axial tumor mass (oligodendroglioma WHO II/IV), underwent the language task, and relevant cortical activation was observed in the posterior aspect of the right superior temporal gyrus. In this case, clusters of activation cross the sulcus (Fig. 3C). The intraoperative cortical stimulation on the language-related loci (Fig. 3D) resulted in temporary speech arrests during a picture-naming task [Snodgrass and Vanderwart, 1980], validating the fMRI findings. Using intra-operative MR image guidance, a subtotal tumor resection was performed without compromising the patient's language function.

Multiresolution fMRI in a normal subject

Figure 4 shows fMRI results from the healthy volunteer performing the sequential finger-tapping task, and Figure 5 shows the results from the auditory word-matching task.

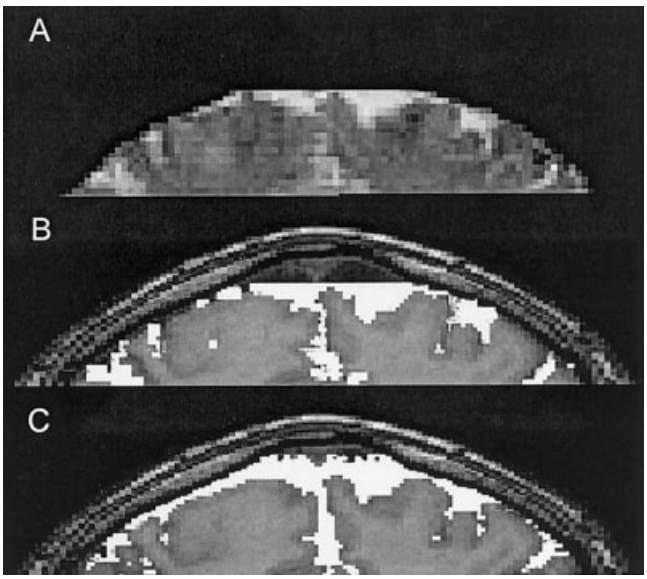

Figure 2.

A: A coronal section from the first set of EPI images acquired in the fMRI experiment. **B:** The EPI image was thresholded to delineate the CSF space and overlaid on the T1-weighted anatomical image. **C:** Overlay of the segmented CSF-space obtained from the T1-weighted anatomical images.

These figures demonstrate how spatial morphology of functional activation is obscured by low-resolution data acquisition. For example, the activation of the motor area detected at low resolution, as shown in Figure 4C (see arrow), was grossly extended over the central sulcus, making it impossible to determine if the activation is on both sides of the sulcus or primarily on one side or the other. With an increase in spatial resolution to the intermediate resolution of $3 \times 3 \times 3$ mm^3, the activation still appears to cross over the sulcus (Fig. 4D).

At the highest spatial resolution of $2 \times 2 \times 2$ mm^3 (Fig. 4E), the activation is localized antero-inferior to the central sulcus, suggesting the anticipated involvement of the primary motor area. Based on a qualitative evaluation of the spatial accuracy in registration (demonstrated in Fig. 2), we were able to conclude that mis-registration was not the cause of the apparent localization of activation to the cortical gray matter. Figure 4F shows the result when the highest resolution data are spatially smoothed to have the resolution roughly equivalent to the low-resolution data. Again the activation appears to cross the sulcus, resulting in ambiguity about the gyrus on which the activation can be localized. Figure 4F together with Figure 4C demonstrate clearly that the ambiguity in this case is due to spatial smoothing effects (caused either by low-pass filtering high resolution data or by acquiring data at lower resolution). Note that the slight disparities in activation patterns between Figure 4C and 4F are expected considering that the data were acquired in two separate fMRI runs. It is well known that activation patterns can vary considerably from scan to scan [Rombouts et al., 1998].

A similar trend to that seen in the motor task results was also found in the auditory word-matching task. The regions-of-interest located near the border of the transverse temporal gyrus and inferior parietal lobe are conjoined as a single large activation loci distributed across the lateral fissure in the low-resolution result (Fig. 5C). This spatial obscurity in the activation was significantly reduced by the subsequent

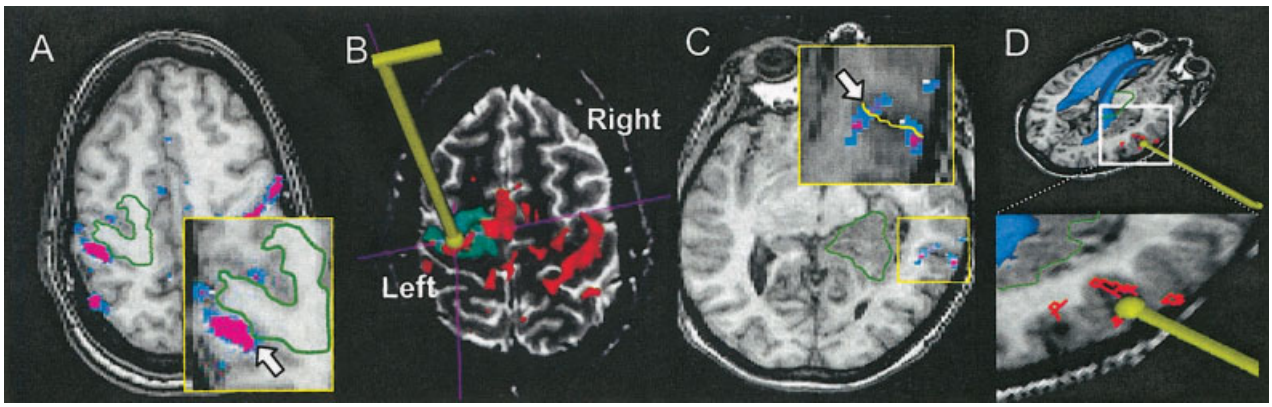

Figure 3.

A: The functional map from Subject 1 (33/F) in axial view (with overlay threshold $P < 10^{-6}$). The tumor boundary is delineated with a green line overlaid on the images. Activation was observed adjacent to the border of a tumor in the precentral gyrus (see arrow). **B:** Intra-operative view seen by the surgical team. The location of the cortical stimulator is shown by placement of a 3-D rendered wand in the image. Eloquent motor areas are shown in red. **C:** The functional map from Subject 2 (34/F) in axial view. Activation is observed at the boundary between two adjacent gyri, i.e., inferior aspect of STG and the superior aspect of MTG (arrow). **D:** Intra-operative view seen by the surgical team. Intra-operative cortical stimulation identified speech/language areas in the right posterior superior temporal lobe as shown.

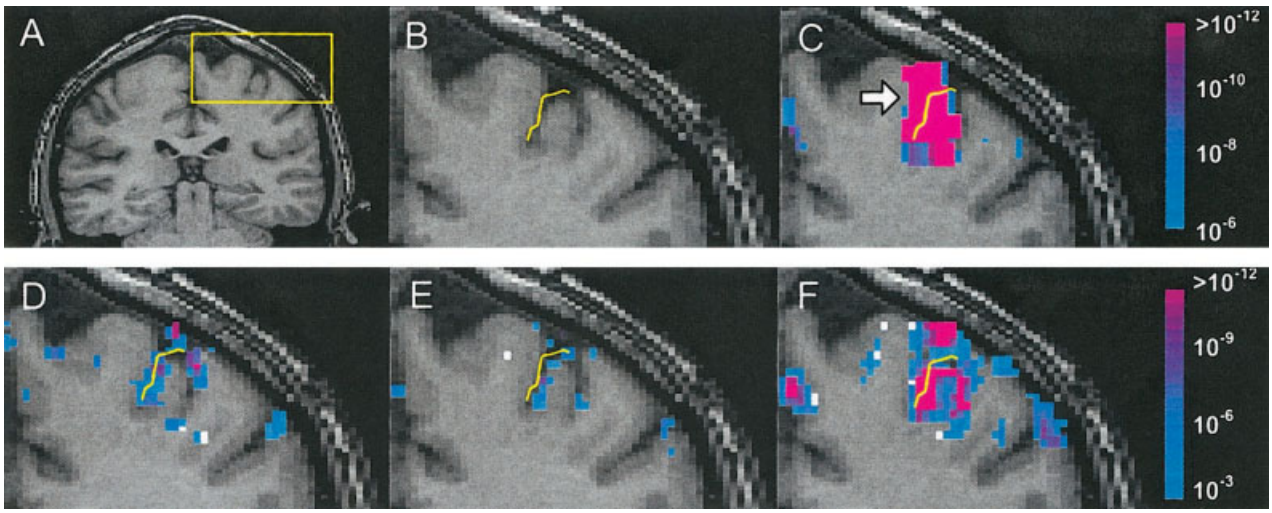

Figure 4.

Results from motor fMRI study of normal subject. **A:** Subject's coronal anatomy with region-of-interest (see box) in motor-related functional area. **B:** Delineation of the central sulcus. (**C**) Low, (**D**) intermediate, and (**E**) high spatial resolution functional maps obtained from data according to the protocols described in Table II. **F:** Functional map obtained from high spatial resolution data that were spatially smoothed to the equivalent level of the low-resolution data.

data acquisition at higher spatial resolutions (Fig. 5D,E), where the activation was localized to the superior bank of transverse temporal gyrus (primary auditory area). Note that in this case, the intermediate resolution of $3 \times 3 \times 3$ mm^3 (Fig. 5D) appears to be sufficient to unambiguously localize the activation. Again, smoothing the high-resolution data causes the activation to appear to extend across the lateral fissure in the superior-inferior direction (Fig. 5F).

DISCUSSION

The outcome of low-grade and high-grade glioma surgery correlates with the extent of surgical resection [Berger et al., 1994; Keles et al., 2001; Lacroix et al., 2001]. Therefore, a principal goal of surgery in these cases is to achieve maximum tumor resection. However, given the need to insure the preservation of neurological function, determining the

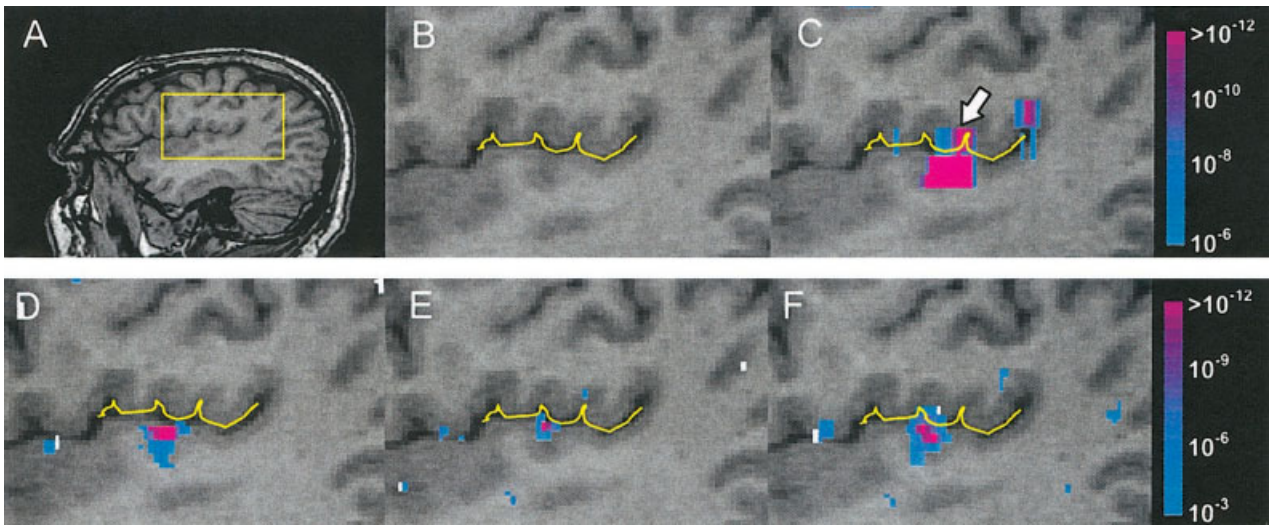

Figure 5.

Results from language fMRI study of normal subject. **A:** Subject's sagittal anatomy with region-of-interest (see box) at the border of primary auditory areas and inferior parietal lobe. **B:** Delineation of lateral fissure. (**C**) Low, (**D**) intermediate, and (**E**) high spatial resolution functional maps obtained from data according to the protocols described in Table II. **F:** Functional map obtained from high spatial resolution data that was spatially smoothed to the equivalent level of the low-resolution data.

extent of resection and the optimal surgical corridor to the lesion can be difficult. The value of imaging in this context cannot be understated. Approaches combining both intra-operative and pre-operative imaging, including functional MRI, have been employed in order to provide a surgical navigation tool [Gering et al., 2001; Nabavi et al., 2001; Roux et al., 2001].

To be useful for surgical planning and guidance, accuracy in delineation of the functional activation with respect to the surgical anatomy is clearly necessary. However, determining the exact relationship between fMRI results and neuroanatomy as well as the impact of this relationship on surgical outcome is an enormously difficult task. One of the approaches used in this study has been to query the neurosurgical expert regarding the potential ambiguity in fMRI results via examinations of a series of surgical cases. The conclusion of this study is that accuracy in surgical planning and execution could be improved if fMRI was able to unambiguously predict which gyri should be avoided in the surgical approach to the lesion.

In our review of the recently reported fMRI investigations for neurosurgical planning, we found a wide range of resolution parameter settings (Fig. 1) with little or no justification for their use with respect to the goals of surgical planning. The voxel sizes that have been used have typically been significantly greater than $3 \times 3 \times 3$ mm^3. In this report, based on an examination of the results from eight patients, we have shown qualitatively that a spatial resolution of $3.75 \times 3.75 \times 4$ mm^3, which is slightly higher than that used in most fMRI data acquisitions for surgical planning, can cause ambiguity significant enough to impact surgical decision making.

Our studies suggest that a relatively high spatial resolution may be needed for the unambiguous identification of cortical activation with respect to tumors and important anatomical landmarks. The thickness of gray matter in humans is on average approximately 2.5 mm, and varies between 1 to 4.5 mm [Fischl and Dale 2000]; thus, 2-mm resolution would seem to be a reasonable choice in order to keep activation loci from extending beyond their biological boundaries. Furthermore, given the complex folding of the cortex, isotropic voxels are most appropriate. Indeed, from our fMRI studies on a normal volunteer, data acquired at a 2-mm isotropic resolution is sufficient to constrain activation within cortical areas. However, data acquired at a 3-mm isotropic resolution could still cause ambiguity. For example, activation appeared on both sides of a sulcus at 3-mm resolution (Fig. 4D) while it was clearly located on only one side only when the resolution was increased to 2 mm (Fig. 4E).

An important theoretical concern is that whether it is actually possible to determine which side of a sulcus is giving rise to an observed signal since BOLD signals, particularly at low field such as 0.5T, tend to arise predominantly from larger caliber vessels that may be located within the sulcus rather then in the cortical parenchyma [Gati et al., 1997; Krings et al., 1999; Menon et al., 1995]. One of the main advantages of high-field fMRI, 3T and higher, is that the portion of signals originating from parenchymal activation becomes greater than the contribution from large veins and venuoles [Menon et al., 1995]. In cases such as surgical planning, where high-spatial resolution is necessary to achieve precise delineation of activation boundaries, acquiring data at high field strength will also significantly improve BOLD contrast [Menon et al. 1995].

Unfortunately, increasing spatial resolution also reduces signal-to-noise ratio (SNR) and detectability of functional activation generally suffers. We have previously reported the results of detailed theoretical and experimental analyses of the relationship between spatial resolution and detectability of functional activation as measured by BOLD contrast-to-noise ratio [Chen et al., 2003; Yoo et al., 2001]. From our previous analysis, we would conclude that, given the SNR penalty, high spatial resolution data acquisition is not necessarily advantageous for many neuro-scientific investigations. For example, precise delineation of activation boundaries is of limited use when data is eventually normalized and averaged over subject populations. Nor would high resolution be important for fMRI-based language/memory lateralization tests for patients with intractable temporal lobe epilepsy [Deblaere et al., 2002; Golby et al., 2002] because high resolution is not relevant to the hemispheric localization of language/memory function.

Even at higher field strength, activation in some regions may be difficult to detect with voxels as small as 2 mm. Multiresolution detection approaches can be employed for processing high-resolution data. For example, the data can be spatially smoothed and processed at multiple resolutions to detect regions of activation [Brammer, 1998]. Although it is always possible to perform multiresolution processing on high-resolution data to optimize the SNR for detection of activation, it cannot be assumed that there is no SNR penalty to be paid for high-resolution data acquisition. High-resolution acquisitions require longer imaging times to cover the same volume, thus, SNR is lower at high-resolution not only because voxels are smaller but because fewer acquisitions can be made during an fMRI scanning session. For example, using a 3-mm slice thickness, only one half of the volume acquisitions can be made during an fMRI session of fixed time as compared to the number of acquisitions that can be made if a 6-mm slice thickness is used. In such a case, the reduction in the number of acquisitions results in a reduction of about 30% in SNR on top of the reduction due to the smaller voxel size.

There is an optimal resolution at which fMRI data should be acquired for any given goal [Chen et al. 2003; Yoo et al., 2001]. Resolution must be high enough to satisfy fundamental goals of the experiment, e.g., to permit precise delineation of activation loci with respect to tumor boundaries. On the other hand, the acquisition resolution should not be too high, otherwise low SNR may result in obscuring of activation boundaries by excessive noise or, if SNR is very low, even cause activation loci to be missed altogether.

To optimize fMRI acquisition with respect to spatial resolution, we have investigated a real-time adaptive acquisition approach whereby the fMRI scan session is divided into multiple scan stages [Yoo et al., 1999]. In the first scan stage, detection of eloquent functional regions-of-interest is done at low resolution. In subsequent scan stages, higher resolution data are acquired in a restricted volume (selected by examining the lower-resolution results). Because the high-resolution acquisition stage covers only a restricted volume, the number of acquisitions per unit time is not greatly impacted by increasing spatial resolution. Consequently, SNR is enhanced compared to a whole-volume, high-resolution acquisition. The optimization of imaging parameters necessary for adaptive multiresolution fMRI, in the context of neurosurgical planning, is an active area of research and development in our laboratory.

ACKNOWLEDGMENTS

We thank Xingchang Wei, Heather O'Leary, and Gauri Paralkar for assistance with data acquisition and processing.

REFERENCES

Berger MS, Deliganis AV, Dobbins J, Keles GE (1994): The effect of extent of resection on recurrence in patients with low grade cerebral hemisphere gliomas. Cancer 74:1784–1791.

Bittar RG, Olivier A, Sadikot AF, Andermann F, Pike GB, Reutens DC (1999): Presurgical motor and somatosensory cortex mapping with functional magnetic resonance imaging and positron emission tomography. J Neurosurg 91:915–921.

Brammer MJ (1998): Multidimensional wavelet analysis of functional magnetic resonance images. Hum Brain Mapp 6:378–382.

Chen NK, Dickey CC, Yoo SS, Guttmann CR, Panych LP (2003): Selection of voxel size and slice orientation for fMRI in the presence of susceptibility field gradients: application to imaging of the amygdala. Neuroimage 19:817–825.

Cifelli A, Matthews PM (2002): Cerebral plasticity in multiple sclerosis: insights from fMRI. Mult Scler 8:193–199.

Deblaere K, Backes WH, Hofman P, Vandemaele P, Boon PA, Vonck K, Boon P, Troost J, Vermeulen J, Wilmink J, Achten E, Aldenkamp A (2002): Developing a comprehensive presurgical functional MRI protocol for patients with intractable temporal lobe epilepsy: a pilot study. Neuroradiology 44:667–673.

Fandino J, Kollias SS, Wieser HG, Valavanis A, Yonekawa Y (1999): Intraoperative validation of functional magnetic resonance imaging and cortical reorganization patterns in patients with brain tumors involving the primary motor cortex. J Neurosurg 91:238–250.

Fischl B, Dale AM (2000): Measuring the thickness of the human cerebral cortex from magnetic resonance images. Proc Natl Acad Sci USA 97:11050–11055.

Gati JS, Menon RS, Ugurbil K, Rutt BK (1997): Experimental determination of the BOLD field strength dependence in vessels and tissue. Magn Reson Med 38:296–302.

Gering DT, Nabavi A, Kikinis R, Hata N, O'Donnell LJ, Grimson WE, Jolesz FA, Black PM, Wells WM, III (2001): An integrated visualization system for surgical planning and guidance using image fusion and an open MR. J Magn Reson Imag 13:967–975.

Golby AJ, Poldrack RA, Illes J, Chen D, Desmond JE, Gabrieli JD (2002): Memory lateralization in medial temporal lobe epilepsy assessed by functional MRI. Epilepsia 43:855–863.

Hanakawa T, Ikeda A, Sadato N, Okada T, Fukuyama H, Nagamine T, Honda M, Sawamoto N, Yazawa S, Kunieda T, Ohara S, Taki W, Hashimoto N, Yonekura Y, Konishi J, Shibasaki H (2001): Functional mapping of human medial frontal motor areas. The combined use of functional magnetic resonance imaging and cortical stimulation. Exp Brain Res 138:403–409.

Hirsch J, Ruge MI, Kim KH, Correa DD, Victor JD, Relkin NR, Labar DR, Krol G, Bilsky MH, Souweidane MM, DeAngelis LM, Gutin PH (2000): An integrated functional magnetic resonance imaging procedure for preoperative mapping of cortical areas associated with tactile, motor, language, and visual functions. Neurosurgery 47:711–721.

Howard MW, Kahana MJ (2001): When does semantic similarity help episodic retrieval? J Memory Lang 46:85–98.

Keles GE, Lamborn KR, Berger MS (2001): Low-grade hemispheric gliomas in adults: a critical review of extent of resection as a factor influencing outcome. J Neurosurg 95:735–745.

Kober H, Nimsky C, Moller M, Hastreiter P, Fahlbusch R, Ganslandt O (2001): Correlation of sensorimotor activation with functional magnetic resonance imaging and magnetoencephalography in presurgical functional imaging: a spatial analysis. Neuroimage 14:1214–1228.

Krings T, Erberich SG, Roessler F, Reul J, Thron A (1999): MR blood oxygenation level-dependent signal differences in parenchymal and large draining vessels: implications for functional MR imaging. Am J Neuroradiol. 20:1907–1914.

Krings T, Schreckenberger M, Rohde V, Foltys H, Spetzger U, Sabri O, Reinges MH, Kemeny S, Meyer PT, Moller-Hartmann W, Korinth M, Gilsbach JM, Buell U, Thron A (2001): Metabolic and electrophysiological validation of functional MRI. J Neurol Neurosurg Psychiatry 71:762–771.

Lacroix M, Abi-Said D, Fourney DR, Gokaslan ZL, Shi W, DeMonte F, Lang FF, McCutcheon IE, Hassenbusch SJ, Holland E, Hess K, Michael C, Miller D, Sawaya R (2001): A multivariate analysis of 416 patients with glioblastoma multiforme: prognosis, extent of resection, and survival. J Neurosurg 95:190–198.

Lowe A, Williams S, Symms M, Stolerman I, Shoaib M (2002): Functional magnetic resonance neuroimaging of drug dependence: naloxone-precipitated morphine withdrawal. Neuroimage 17:902–910.

Menon RS, Ogawa S, Hu X, Strupp JP, Anderson P, Ugurbil K (1995): BOLD based functional MRI at 4 Tesla includes a capillary bed contribution: Echo-Planar Imaging correlates with previous optical imaging using intrinsic signals. Magn Reson Med 33:453–459.

Nabavi A, Black PM, Gering DT, Westin CF, Mehta V, Pergolizzi RS Jr, Ferrant M, Warfield SK, Hata N, Schwartz RB, Wells WM 3rd, Kikinis R, Jolesz FA (2001): Serial intraoperative magnetic resonance imaging of brain shift. Neurosurgery 48:787–797.

Nimsky C, Ganslandt O, Kober H, Buchfelder M, Fahlbusch R (2001): Intraoperative magnetic resonance imaging combined with neuronavigation: a new concept. Neurosurgery 48:1082–1089.

Ojemann JG, Miller JW, Silbergeld DL (1996): Preserved function in brain invaded by tumor. Neurosurgery 39:253–258.

Pouratian N, Bookheimer SY, Rex DE, Martin NA, Toga AW (2002a): Utility of preoperative functional magnetic resonance imaging for identifying language cortices in patients with vascular malformations. J Neurosurg 97:21–32.

Pouratian N, Sicotte N, Rex D, Martin NA, Becker D, Cannestra AF, Toga AW (2002b): Spatial/temporal correlation of BOLD and optical intrinsic signals in humans. Magn Reson Med 47:766–776.

Rohlfing T, West JB, Beier J, Liebig T, Taschner CA, Thomale UW (2000): Registration of functional and anatomical MRI: accuracy assessment and application in navigated neurosurgery. Comput Aided Surg 5:414–425.

Rombouts SA, Barkhof F, Hoogenraad FG, Sprenger M, Scheltens P (1998): Within-subject reproducibility of visual activation patterns with functional magnetic resonance imaging using multislice echo planar imaging. Magn Reson Imag 16:105–113.

Roux FE, Ibarrola D, Tremoulet M, Lazorthes Y, Henry P, Sol JC, Berry I (2001): Methodological and technical issues for integrating functional magnetic resonance imaging data in a neuronavigational system. Neurosurgery 49:1145–1156.

Schiffbauer H, Ferrari P, Rowley HA, Berger MS, Roberts TPL (2001): Functional activity within brain tumors: a magnetic source imaging study. Neurosurgery 49:1313–1321.

Schlosser MJ, Luby M, Spencer DD, Awad IA, McCarthy G (1999): Comparative localization of auditory comprehension by using functional magnetic resonance imaging and cortical stimulation. J Neurosurg 91:626–635.

Skirboll SS, Ojemann GA, Berger MS, Lettich E, Winn HR (1996): Functional cortex and subcortical white matter located within gliomas. Neurosurgery 38:678–684.

Snodgrass JG, Vanderwart M (1980): A standardized set of 260 pictures: norms for name agreement, image agreement, familiarity, and visual complexity. J Exp Psychol [Hum Learn] 6:174–215.

Wells WM 3rd, Viola P, Atsumi H, Nakajima S, Kikinis R (1996): Multi-modal volume registration by maximization of mutual information. Med Image Anal 1:35–51.

Yoo SS, Guttmann CR, Zhao L, Panych LP (1999): Real-time adaptive functional MRI. Neuroimage 10:596–606.

Yoo SS, Guttmann CR, Panych LP (2001): Multiresolution data acquisition and detection in functional MRI. Neuroimage 14: 1476–1485.